*Cellular and Molecular Biology*™ **46** (5), 871-882
Printed in France.

0145-5680/00
2000 Cell. mol. Biol.™

# TARGETING EXPOSED RNA REGIONS IN CRYSTALS OF THE SMALL RIBOSOMAL SUBUNITS AT MEDIUM RESOLUTION

Heike BARTELS[1], Marco GLUEHMANN[2], Daniela JANELL[2], Frank SCHLUENZEN[2], Ante TOCILJ[2], Anat BASHAN[1], Inna LEVIN[1], Harly A.S. HANSEN[2], Joerg HARMS[2], Maggie KESSLER[1], Marta PIOLETTI[3], Tamar AUERBACH[1,4], ILANA AGMON[1], Horacio AVILA[3], Maria SIMITSOPOULOU[3], Shulamith WEINSTEIN[1], Moshe PERETZ[1], William S. BENNETT[2], Francois FRANCESCHI[3] and Ada YONATH[1✍,2]

[1✍] Department of Structural Biology, Weizmann Institute, 76100 Rehovot, Israel
fax *+972 8 934 4154;* e-mail *csyonath@weizmann.weizmann.ac.il*
[2] Max-Planck-Research Unit Ribosomal Structure, Notkestrasse 85, 22603 Hamburg, Germany
[3] Max-Planck-Institute for Molecular Genetics, Ihnestrasse 73, 14195 Berlin, Germany
[4] FU-Berlin, Dept. of Biochememistry and Pharmacology, Takustrasse 3, 14195 Berlin, Germany

*Received August 5, 1999; Accepted September 19, 1999*

**Abstract** - Within the framework of ribosomal crystallography, the small subunits are being analyzed, using crystals diffracting to 3 Å resolution. The medium resolution electron density map of this subunit, obtained by multiple isomorphous replacement, show recognizable morphologies, strikingly similar to the functional active conformer of the small ribosomal subunit. It contains elongated dense features, traceable as RNA chains as well as globular regions into which the structures determined for isolated ribosomal proteins, or other known structural motifs were fitted. To facilitate unbiased map interpretation, metal clusters are being covalently attached either to the surface of the subunits or to DNA oligomers complementary to exposed ribosomal RNA. Two surface cysteines and the 3' end of the 16S ribosomal RNA have been localized. Targeting several additional RNA regions shed light on their relative exposure and confirmed previous studies concerning their functional relevance.

**Key words**: Ribosomes, crystallography of 16S RNA, cDNA, anti-Shine-Dalgarno

**Abbreviations**: **70S, 50S, 30S**: the whole ribosome and its two subunits from prokaryotes, respectively. A letter prefix to the ribosomal particles or ribosomal proteins represents the bacterial source (e.g. E: *Escherichia coli*; T: *Thermus thermophilus*). The names of the ribosomal proteins are composed of a prefix showing the bacterial source, the letters L or S, showing that this protein is of the large or small subunit, and a running number, according to sequence homology considerations. **MIR**: multiple isomorphous replacement; **SIRAS** and **MIRAS**: single and multiple isomorphous replacement combined with anomalous scattering; **TAMM**: tetrakis(acetoxymercuri)-methane; **TIR**: tetrairidium cluster.

## INTRODUCTION

Ribosomes are the universal cell organelles facilitating the translation of the genetic code into polypeptide chains. They are nucleoprotein assemblies, built of two independent subunits of unequal size which associate upon the initiation of protein biosynthesis. The large subunit catalyzes the formation of the peptide bond and provides the path for the progression of the nascent proteins. The small subunit is responsible for the initiation step of the

translation process and facilitates the decoding of the genetic information. The molecular weights of bacterial ribosomes and their large and small subunits are 2.3 mDa, 1.45 mDa and 0.85 mDa, respectively. About one third of the bacterial ribosomal mass comprises of some 58-73 different proteins, depending on its source. The remaining two thirds are three chains of rRNA, of a total of about 4500 nucleotides.

Crystals diffracting to about 3 Å have been grown from the small and the large subunits, despite their unfavorable properties, namely their enormous size, lack of internal symmetry, inherent flexibility and a surface composed of highly degradable RNA alongside with proteins which may be loosely held. The extremely weak diffraction power of all ribosomal crystals dictates absolute dependance on synchrotron radiation. At cryo temperature, complete diffraction data sets can be collected with moderate beam intensity at medium resolution, but, quality data at the higher resolution shells, i.e. beyond 4.5-5 Å, can be collected only with brighter beam. However, under these conditions the ribosomal crystals show severe radiation sensitivity even at He-stream temperatures, 15-25 K. Thus, resolution decay from 3 to 6 Å is usually detected within a period sufficient for covering only 1-1.5 degrees of rotation (Krumbholz *et al.*, 1998; Yonath *et al.*, 1998). Nevertheless, procedures were developed to minimize the harm, thus overcoming part of the decay problem. Consequently, well behaved data sets were obtained for the diffraction of native and derivatized crystals to 3-3.5 Å resolution, and an interpretable electron density map of the small ribosomal subunit from *T. thermophilus* (T30S) was constructed at 4.5 Å.

The 7 Å (Schluenzen *et al.*, 1999) and the 4.5 Å (Tocilj *et al.*, 1999) electron density maps reveal recognizable morphologies, remarkably similar to that seen in EM reconstructed of the functionally active conformer of the small subunit (Harms *et al.*, 1999; Gabashvili *et al.*, 1999). It contains elongated dense regions, spanning the particles in different directions as well as globular patches of lower density, readily distinguishable from the above. It was partially interpreted by fitting known structural motifs of RNA and proteins. In this way, secondary structure elements, such as RNA single strands and duplexes have been pinpointed. In parallel, regions into which domains of ribosomal proteins could be fitted, have been identified (Bashan *et al.*, 1999; Schluenzen *et al.*, 1999).

Nevertheless, considerable uncertainties are associated with the placements of structures determined for isolated ribosomal components into the medium resolution maps of the entire ribosomal particles. These are connected to the ambiguities that are likely to accompany fittings of the frequently occurring structural motifs (Liljas and Al-Karadaghi, 1997; Ramakrishnan and White, 1998) into medium resolution maps, as well as from the non-negligible conformational variability of the ribosomal components and from the possible influences of the proximity to other r-proteins or rRNA on the *in situ* conformations. Therefore we have focused on inserting heavy atom markers to natural or genetically engineered predetermined sites (Auerbach *et al.*, 1999; Simitsopoulou *et al.*, 1999).

In this manuscript we highlight the targeting of exposed cysteines belonging to two ribosomal proteins as well as selected ribosomal RNA regions. For the latter, markers made of heavy atom compounds bound to DNA oligomers complementary to the exposed ribosomal RNA regions, have been exploited. We describe the localizations of some of these markers in the electron density map of the small ribosomal subunit from *Thermus thermophilus*. Possible structural and functional implications are also being discussed.

## RESULTS AND DISCUSSION

### *About the medium resolution map of the small ribosomal subunit*

The small ribosomal subunits exhibit the lowest level of stability and the highest level of flexibility and

heterogeneity among the ribosomal particles (Berkovitch-Yellin *et al.*, 1992; Gabashvili *et al.*, 1999). Multi conformational states were suggested to account for the inconsistencies in locations of selected components revealed by surface probing (Alexander *et al.*, 1994; Wang *et al.*, 1999) or by monitoring the ribosomal activity (Camp and Hill, 1987; Weller and Hill, 1992). Indeed, the early T30S crystals (Trakhanov *et al.*, 1989; Yonath *et al.*, 1988) yielded satisfactory data only to 10-12 Å resolution (Schluenzen *et al.*, 1995).

Crystals of T30S diffracting to rather high resolution 3-3.5 Å, are obtained routinely in our laboratories. More quality crystals were detected when the proportion of the active conformation of the 30S particles was increased in the crystallization droplet or within the crystals by selected additives (Tocilj *et al.*, 1999). Alternatively, the increase in quality was achieved by the crystallization of ribosomal particles trapped in their activation state (by chemical methods) or complexed with antibiotics, such as edeine (Szer and Kurylo-Borowska, 1972), that are known to "freeze" the 30S subunits at a particular conformational state (Moazed and Noller, 1987). Although a reasonable part of the native T30S crystals that are currently being grown, diffract to around 3 Å resolution, lower resolution (i.e. 4.5-8 Å) has been observed for some of the heavy atom derivatives that were obtained by soaking.

Careful interplay between heavy atom clusters, organo-metallic compounds and heavy metal salts, combined with step-wise addition of phase improvement obtained by density modification procedures, led to a medium resolution (7 Å) map of T30S (Yonath *et al.*, 1998; Bashan *et al.*, 1999; Harms *et al.*, 1999; Schluenzen *et al.*, 1999). This map contains morphologies remarkably similar to most of the EM reconstructions of the small subunits with their recognizable features, with the traditional division of the 30S subunit into three main parts: a head, a rather narrow neck and a bulky lower body (Frank *et al.*, 1995; Stark *et al.*, 1995; Lata *et al.*, 1996; Gabashvili *et al.*, 1999). Visual examination indicated that the conformer within the T30S crystals resembles that seen in functionally active 70S ribosomes more than that of free particles.

Internal features of the 7 Å map include dense elongated chains that span the 30S particle in various directions and show features similar to those detected in nucleosome core particles at comparable resolution (Richmond *et al.*, 1984). About half of these have been traced either as separated RNA duplexes or as single RNA strands (Fig. 1), showing an overall tertiary organization remarkably similar to that postulated for the RNA duplexes by incorporating biochemical, foot-printing and crosslinking data into the cryo EM reconstruction (Mueller and Brimacombe, 1997). Readily distinguishable regions of lower density could be assigned to folds observed in isolated r-proteins by NMR and crystallography at atomic resolution, using the main chain coordinates as templates. For their identification, guide lines were taken from the locations suggested in earlier studies, based on immuno electron microscopy and neutron scattering (Stöffler and Stöffler-Meilicke, 1986; Capel *et al.*, 1988; Mueller and Brimacombe, 1997), keeping in mind that such assignments are only partially justified. Several examples are given below.

Protein S15 is of special interest because it belongs to the subset of ribosomal proteins that bind to the 16S RNA independently of other components. This is assumed to provide the nucleus for ribosomal assembly (Held *et al.*, 1974), and also that it was shown to possess a fair amount of conformational flexibility. Thus, NMR and X-ray crystallography investigations, carried out on isolated protein S17 led to almost identical three-dimensional structure of the helical core of this protein, but at the same time, significant conformational deviations were observed in the remaining alpha helix (Berglund *et al.*, 1997, Clemons *et al.*, 1998). Indeed, the core of this protein could be placed in the 7 Å map in several positions. In all less density was found at the location where the flexible arm should have been positioned if the crystallographic structure determined in isolation is maintained within the ribosomes (Schluenzen *et al.*, 1999).

All available crystal structures of ribosomal proteins belonging to the small subunit, were fitted into the 7 Å map, with no alterations (Figs. 2-4 and in Bashan *et al.*, 1999). These include proteins TS5 (Ramakrishnan and White, 1992), TS6 (Lindhal *et al.*, 1994), TS7 (Hosaka *et al.*, 1997; Wimberly *et al.*, 1997; Tanaka *et al.*, 1998), TS8 (Davies *et al.*, 1996; Nevskaya *et al.*, 1998), TS15 (Clemons *et al.*, 1998) and TS17 (Golden *et al.*, 1993). Among them, protein TS5 (Fig. 3) is of special importance for our studies, as it is being used as a vehicle for the introduction of a relative large number of seleniums into the small subunit, for MAD phasing at high resolution (Auerbach *et al.*, 1999).

Inspection of the interactions between the various ribosomal components revealed several architectural elements with significant diversity in their modes of recognition, as found for smaller protein: RNA complexes (summarized by Cusack, 1999; Draper and Reynoldo, 1999). For example, hints showing that ribosomal proteins may stabilize the three-dimensional fold of rRNA chains were detected in several locations of the map (Bashan *et al.*, 1999).

*Heavy atom targeting*

The 7 Å map has been extended to 5 Å resolution by computational methods. Examination of the latter showed clearly that even this resolution is still not sufficient for reliable interpretation at the molecular level. For this, higher resolution and improved phases are essential. As several heavy atoms derivatives that diffract to 3.5 Å and seem to possess suitable phasing power, have been recently identified, further interpretation has been deferred to later stages. Furthermore, although the fitting of known structures to prominent features of the available maps led to interesting findings, the subjective nature of them should not be overlooked.

Less biased and more accurate positioning of the ribosomal components poses additional challenges and requires independent structural information. To flag specific positions, markers inserted in pre-determined sites are being exploited. These are composed of heavy atom compounds that are attached either directly to the ribosomal particles via chemically reactive moieties located at their surface or to carriers that bind to the ribosomal particles specifically with a high affinity. For obtaining high occupancies of the heavy atom markers, covalent binding with a high yield is preferred.

Two tetra-metal compounds, namely tetrakis (acetoxymercuri)-methane (TAMM) and a tetrairidium cluster (TIR), are being used for this aim. TIR is composed of an internal core of four iridium atoms, with a diameter of 4.8 Å (Jahn, 1989). In order to increase its stability and solubility in aqueous solutions, it is surrounded by a shell of organic moieties of chemical composition similar to that of proteins. To facilitate the binding of this cluster to the ribosomal moieties, a chemically reactive bridging arm, designed to bind to free sulfhydryl groups, has been attached to it. To reduce the potential flexibility of this marker, this bridging arm was designed with a minimal length and maximal stability. Consequently, this arm is slightly longer than the longest amino acid side chain, and contains an amide bond. Hence, the expectations for local rather rigid conformations proved to be legitimate (Weinstein *et al.*, 1999).

TAMM, a tetra-mercury compound, was the key compound for phasing the data obtained from crystals of several biological compounds (e.g. the nucleosome-core particle (Luger *et al.*, 1997), the photosynthetic reaction center (Deisenhofer *et al.*, 1984), an idiotope-anti-idiotype complex (Bentley *et al.*, 1990) and glutathione transferase (Reinemer *et al.*, 1991). It is somewhat less compact than TIR, but binds directly to available -SH moieties, thus eliminating the concern about the flexibility, the length and the chemical reactivity of bridging arms.

Suitable candidates for binding the heavy atom compounds may be ribosomal proteins, antibiotics, complementary DNA (cDNA) oligomers, charged tRNA molecules, antibodies raised against selected ribosomal moieties (Auerbach *et al.*, 1999) and factors participating in the translation process.

*Flagging two surface ribosomal proteins*

Labeling studies carried out on T30S particles in solution indicated one fully and one partially exposed SH groups (Sagi *et al.*, 1995). These were found to belong to the cysteines of proteins TS11 (residue 119) and TS13 (residue 84) (Wada *et al.*, 1999). TIR was bound to these -SH groups prior to the crystallization of the 30S subunits. The crystals obtained from these modified particles diffract to 4.5 Å resolution and found to be isomorphous with the native ones. This may indicate that while in the crystal, the motion of the bridging arm is limited despite its potential flexibility.

The attachment of 1-2 equivalents of TIR yielded a weak derivative, albeit a rather powerful marker. Two prominent peaks were revealed in difference Fourier maps (signal to noise values of 3.9 and 4.5), using the amplitudes of the data collected from the TIR modified crystals with the MIR phases of T30S (Weinstein *et al.*, 1999). The crystallographically determined minor site of the TIR compound (Fig. 5) was found to be on the particle's "head", in a position similar to that of protein S13, as revealed by immuno electron microscopy (Stöffler and Stöffler-Meilicke, 1986), neutron scattering (Capel *et al.*, 1988) and modeling (Mueller and Brimacombe, 1997).

The major site, assigned as the cysteine of TS11, is located at the central part of the particle, in a position roughly compatible with that suggested by immuno electron microscopy for protein S11 in E30S (Stöffler and Stöffler-Meilicke, 1986) as well as that suggested by modeling the ribosomal components within cryo-EM reconstructions (Mueller and Brimacombe, 1997). However, it deviates by approximately 35 Å from the position assigned to the center of mass of this protein by triangulation studies exploiting neutron scattering and contrast variation (Capel *et al.*, 1988). Since both the tetrairidium cluster and the immuno electron microscopy target the surface of the ribosomal particles, whereas the triangulation method approximates the positions of the centers of mass of the ribosomal proteins, such inconsistency should be tolerable. It may also stem, partially or fully from the internal flexibility of the small subunit and its multi-conformer nature, as was suggested for the deviation of 65 Å detected between the triangulation localizations and those exploiting complementary DNA (Alexander *et al.*, 1994).

The bridging arm of TIR was designed to bind almost exclusively to exposed -SH groups. The specificity of TAMM is somewhat lower. It has high preference to sulfhydryls, but can also bind to other amino acids, such as histidines. Therefore it is not surprising that more than two peaks (with signal to noise levels larger than 4.5) were detected in different Fourier maps. Among those, one was found in proximity to the prominent Ir peak, in a distance that may be accounted by the length of the bridging arm that was attached to the TIR cluster, but does not exist in TAMM, which binds directly.

Recombinant methods are being exploited to facilitate covalent binding at additional selected locations by extensive insertion of sulfhydryl groups. Since totally reconstituted particles do not yield well diffracting crystals, even when the ribosomal original components are being used, procedure for reversible detachment of selected ribosomal proteins, by chemical, mutations or gene knockouts methods, have been established (Auerbach *et al.*, 1999; Simitsopoulou *et al.*, 1999).

*Surface RNA hybridizations*

DNA oligomers are being exploited for the derivatization of ribosomal crystals and for flagging the locations of the regions of the ribosomal RNA targeted by them. Previous solution studies, focusing at mapping parts of the surface of the *E. coli* ribosomal RNA, have been carried out in solution for over a decade (Oakes *et al.*, 1986; Tapprich and Hill, 1986; Ricker and Kaji 1991; Weller and Hill, 1992; Alexander *et al.*, 1994; Wang *et al.*, 1999). In these procedures synthetic oligodeoxy-nucleotide probes, complementary to selected rRNA sequences, are hybridized to the ribosomal particles and alterations in the activity and in the binding properties are monitored.

These procedures have been extended for rRNA

targeting within the crystals of T30S. The length of the oligodeoxynucleotides (cDNA) is designed to increase the stability of the expected hybrid double helices and the oligomers are being chosen according to their specificity and affinity to bind to the thermophilic subunits, as determined in solution (Table 1). Those that hybridize well are being diffused into native T30S crystals. Their influence on the internal order of the crystals is used as an indicator for the extent of exposure of their complementary rRNA. The oligomers that do not cause substantial resolution drop are modified by heavy atoms. Two approaches are being taken: direct mercuration, via their cytidines or at their terminal phosphates (Auerbach *et al.*, 1999; Schluenzen *et al.*, 1999), or by binding to thiolated nucleotides that have been inserted in the cDNA sequence. After testing the degree of hybridization of the heavy-atom modified DNA oligomers in solution, the oligomers that display a high binding affinity are selected and used in soaking experiments.

**Table 1**

| rRNA region | Extent of binding |
|---|---|
| 3'end* | +++ |
| the decoding region* | +++ |
| 5'end | + |
| H17B | + |
| H31 | + |
| H41 | + |
| H21 | +/- |

* Consistently show near stoichiometric binding, regardless of the preparation or the length of the cDNA oligomer. (Nomenclature adopted from that suggested for the 16S RNA from *E. coli*, according to Brimacombe, 1995).

page 877

**Fig. 1** *RNA regions, as assigned manually into the 7 Å map of T30S, contoured at 1.0 sigma.* Duplexes of 5-7 bases as observed in tRNA (Basavappa and Sigler, 1991) were used as templates.

**Fig. 2** **top**) *One of the regions of the 7 Å that could be assigned to protein TS15 and* (**bottom**) *its location* (circled by an ellipse) *within the part of the 16S RNA that has been fitted to the map so far* (about 560 nucleotides). The electron density available for the positioning of the crystal structure (Clemons *et al.*, 1998) of the protein provides reasonable fit for its core, but less density for its flexible arm, suggesting that the *in situ* structure is closer to that determined in solution (Berglund *et al.*, 1997).

**Fig. 3** *A part of the 7 Å MIR map of T30S in the expected vicinity of protein TS5, contoured at signal to noise level of 0.8 and the X-ray determined structure of the backbone of protein TS5* (Ramakrishnan and White, 1992) *overlaid on it.* Note its contacts with the neighboring rRNA.

**Fig. 4** *Proteins S6* (Lindhal *et al.*, 1994), *S7* (Wimberly *et al.*, 1997; Hosaka *et al.*, 1997), *S8* (Davies *et al.*, 1996; Nevskaya *et al.*, 1998) *and S17* (Golden *et al.*, 1993), *shown as space filling models* (using their crystallographically determined coordinates) *and the parts of the 7 Å map that reside in their vicinity.* The quality of the fit is demonstrated in the bottom raw, showing two helical parts of protein TS7.

**Fig. 5** *The locations of the two bound tetrairidium clusters to one asymmetric unit in the 7 Å map of T30S.* The binding sites (supposed to be the free SH groups of proteins TS11 and TS13) are shown as yellow squares highlighted by arrows. The two particles which are arranged around the crystalllographic two fold axis are shown, but the sites are indicated only on one of them.

**Fig. 6** *The diffraction patterns of T30S crystals into which cDNA oligomers have been diffused.* **a**) The 23 base oligomer to the 3' end of the 16S RNA, containing 3 TAMM molecules at its free end. **b**) The 17 base oligomer, complementary to the 1400 region (no metals were bound to it). The diffraction patterns, each of 0.2 deg rotation, were recorded on MAR 345, at ID2/ESRF. Crystal to detector distance: 570 mm, beam size: 85 x 85 microns, wavelength 0.9887 Å).

**Fig. 7** *The locations of the peaks* (shown as pink spheers overlaid on the 7 Å map of T30S). These peaks were found in a series of different Fourier maps, each constructed from the differences between the diffraction collected from native T30S and the TAMM modified cDNA oligomers, complementary to the 3' end of the 16S RNA, with the 7 Å phase set.

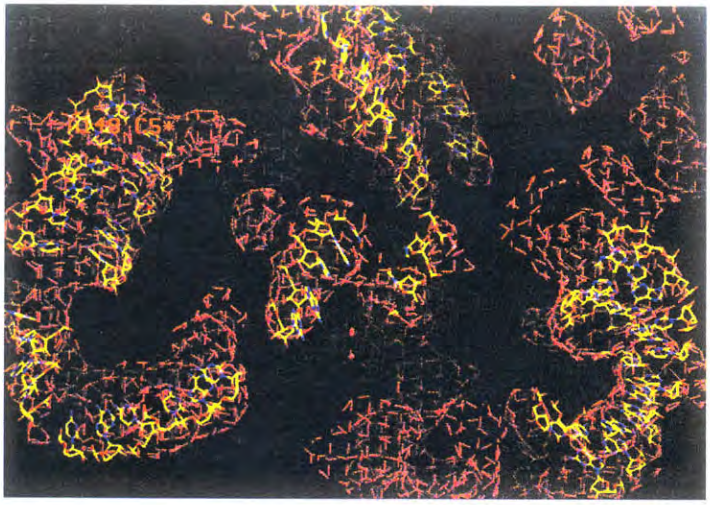

Fig. 1

Fig. 2

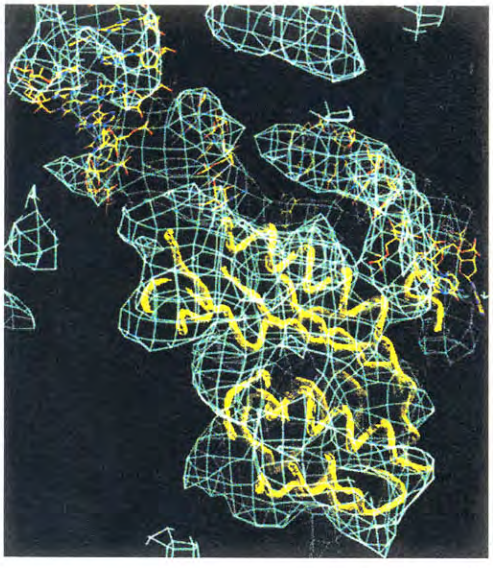

Fig. 3

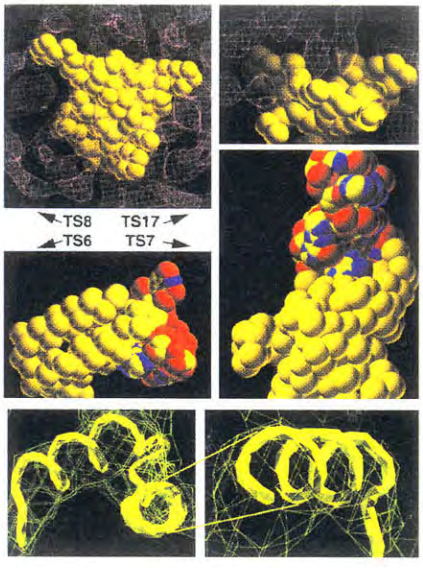


Fig. 4

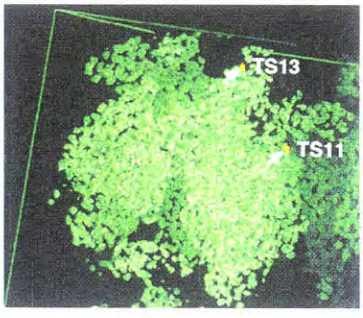


Fig. 5

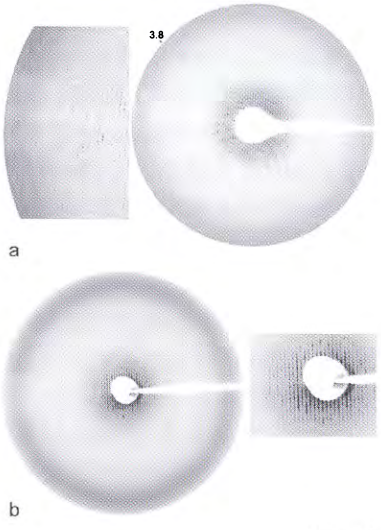


Fig. 6

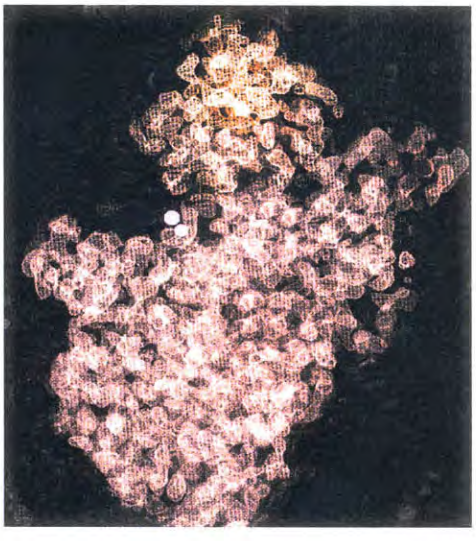

Fig. 7

Soaking crystals in solutions containing the cDNA oligomers into the crystals may provide the answer to the above mentioned problems. Thus, the diffusion is a rather short process, compared to the length of time required for crystallization, and it can be terminated at will by the shock freezing treatment that is applied for data collection, once it is assumed that the hybridization has been completed. In addition, the crystal network utilizes a fair part of the surface of the particle, thus leaving less regions that may compete with the region to which the cDNA was designed. Furthermore, the post-crystallization activation process (Harms *et al.*, 1999; Schluenzen *et al.*, 1999) facilitates the binding of those cDNA oligomers that are designed to mimic functional binding. In general, the volume available within biological crystals for the movement of large heavy atoms is rather limited. Therefore long heavy atom carriers, such as most of the cDNA oligomers that can reach up to 70 Å, are not commonly used in protein crystallography. However, in the case of T30S, the large continuous solvent regions within the crystals (Harms *et al.*, 1999) may allow for the diffusion.

The cDNA oligomers checked for their hybridization within the crystals, target the seven regions of the 16S rRNA mentioned in table 1. Among them, those hybridizing with the 3' end, as well as two regions near helix 41 did not cause crystal damage, allowing data collection to 3.5-3.9 Å (Fig. 6). Those directed to the 5' end and to helix 21 caused a drop of resolution to 6-7 Å, but yielded data with reasonable quality at this limit. Comparison of these observations with the regions of the 16S RNA protected by the 50S subunit within the 70S ribosome (Merryman *et al.*, 1999), support the assumption that the crystal network utilizes part of the exposed regions of the 16S RNA that show high binding abilities.

The oligomer complementary to the 3' end of the 16S RNA is of a high functional relevance as it hybridizes with the region of the 16S rRNA that contains the anti Shine-Dalgarno sequence, namely the region where the mRNA docks into the 30S to allow the formation of the initiation complexes. Shine-Dalgarno is the signal that discriminates between the starting AUG codon and those AUG triplets coding for internal methionines. This consensus sequence, GGAGG, is located in prokaryotic mRNA 2-8 bases before the starting AUG codon. The complementary anti-Shine-Dalgarno sequence, CCUCC, is located at the 3' end of the 16S rRNA, about a 100 bases away from the decoding center.

The 3' end of the 16S RNA is known to be rather flexible and may adopt several conformations, especially upon binding to the large subunit. Thus, significant differences in the cross-linking patterns of ribosomes and of free 30S subunits were observed. For instance, those formed between it and bases in the vicinity of the decoding center (around C1400) in free 30S, were entirely absent in both 70S ribosomes or polysomes. As this region is not involved in interparticle binding (Merryman *et al.*, 1999), it is conceivable that it has other structural roles, in addition to its major contribution to the initiation of protein biosynthesis. The same part of the decoding region that may be crosslinked with the 3' end in free 30S particles, in the 70S ribosomes it may be crosslinked to tRNA. Thus, it seems that the 3' end region is not only the "gate opener" for the mRNA, but also involved in providing the path taken by tRNA on its way into the decoding region. As the cDNA used in these studies contains the Shine-Dalgarno sequence, it is conceivable that the marked improvement in crystal quality upon the hybridization with this cDNA results from stabilization of the flexible 3' arm in a fashion that mimics its binding of mRNA.

This cDNA oligomer was used for derivatization by attaching to its 5' end the sequence A(6-Thio-dG)$_3$ forming a probe with three potential heavy metal binders, each of which was bound to TAMM. Since only one of the four Hg atoms in the TAMM compounds is needed for binding to the thiolated oligonucleotide, the remaining three Hg atoms were masked in order to reduce the risk of inter-molecular crosslinks as well as non-specific binding to ribosomal moieties (Auerbach *et al.*, 1999). Different Fourier analysis with the 7 Å phase-set (Schluenzen *et al.*, 1999) revealed the possible binding sites of the TAMM

molecules that were attached to the cDNA before soaking. In this way a highly probable location for the 5' end of this cDNA oligomer was elucidated (Fig. 7). It is still premature to determine whether this site reflects the position of the 3' end of 16S RNA in the bound or the free conformations of T30S. However, it is noteworthy that the position assigned for the TAMM molecules is in close proximity of the major sites of the poly-anion that led to marked improvement in the crystal quality (from 8-10 to 3 Å resolution).

As mentioned above, binding oligomers to the 5' end of the 16S RNA resulted in a slight decreases of resolution. It has been suggested that this region is located near the particle's neck, in a region known to be rather flexible. Therefore it is conceivable that the resolution drop is caused by subtle movements within this region, induced by the hybridization. More severe destruction was observed by diffusing a DNA oligomer of a sequence complementing the decoding region, around base 1400. These caused a drop in the resolution to 12-15 Å and a dramatic increase in the mosaic spread (Fig. 6). A change in the conformation of the crystallized particles, induced by the attempted hybridization may be a reason for the destruction of the crystal network. Alternatively, the crystal's destruction could be the result of the competition between the cDNA oligomer and the crystal packing network. The growth of well diffracting crystals by co-crystallization with edeine (Szer and Kurylo-Borowska, 1972), an antibiotic that blocks the binding of tRNA to the P-site by interacting with the region close to the decoding site (Moazed and Noller, 1987), indicate that at least part of the decoding region is available for binding within the crystals. An additional reason for the drop in crystal order may be a partial involvement of this domain in the crystal network. In this case, the high affinity of the complementary oligomer to this region may cause its partial penetration into the crowded inter-particle contact area, attempting to hybridize despite steric hindrances, on the expense of the loss of the crystal network.

*Mixed protein/RNA markers*

The risk associated with using the heavy atom modified DNA oligomers for derivatization stems from their dual chemical affinities to specific parts of the ribosome. Thus, the hybridization may be less effective due to the affinity of the heavy atoms to different moieties on the ribosomal proteins (e.g. -SH groups), as they may divert the oligomers to different locations. As mentioned above, a special effort has been made to minimize the chemical reactivity of the heavy atoms that are bound to the DNA oligomers, in order to avoid their binding to undesired positions. However, mixed proteins/RNA markers may be of high interest in other cases. An example are cis-platin and diaqua-cisplatin that in addition to its expected interactions with protein moieties in a fashion similar to that found for other platinum compounds, they should also intercalate into the rRNA strands. Thus, these Pt compounds are known to be efficient intercalator into DNA helices, at specific sequences rich in GG (Reeder *et al.*, 1997), causing local widening and flattening of the minor groove opposite the platinum adduct (Gelasco and Lippard, 1998).

Preliminary results show that by soaking crystals in diaqua-cisplatin the changes in structure factors are larger than what was observed by cisplatin soaking, as expected from the difference in the strength of the interactions that these two compounds make with DNA. In addition, among the binding sites of this compound, as obtained by different Patterson/Fourier techniques, some were detected also in different maps constructed from data obtained from other Pt derivatives (e.g. $K_2PtCl_4$).

## CONCLUSIONS AND PERSPECTIVES

The medium resolution electron density map of the small ribosomal subunit, obtained by experimentally determined phases, shows a particle of an overall shape remarkably similar to those obtained by various cryo-EM reconstructions of the small ribosomal subunits at their active conformation. As this map contains distinct features, feasible assignments of RNA chains and ribosomal proteins were made, based on earlier non-crystallographic studies performed at much lower level of detail by

electron microscopy, modelling and crosslinking.

To increase the level of objectivity and to decrease the bias involved in previously described localizations, a procedure for flagging of selected ribosomal moieties by covalent binding of heavy atom compounds, was designed. Tailor made ligands of a high affinity to the ribosomes, such as antibiotics or complementary DNA to exposed single strand rRNA regions, can also be exploited for targeting and unbiased positioning, thus providing indispensable information required for map interpretation. Since such ligands can be directed to regions involved in functional activities or specific recognitions, the elucidation of the molecular basis for some functional-dynamic aspects, seem to be feasible.

## EXPERIMENTAL PROCEDURES

Crystallization was performed as described earlier (Yonath *et al.*, 1988). Specific mercuration of cDNA oligomers is described in (Auerbach *et al.*, 1999). The data Collection, evaluation and phasing were performed as described (Harms *et al.*, 1999; Schluenzen *et al.*, 1999).

The binding of the tetrairidium cluster and the elucidation of its positions are described in Weinstein *et al.* (1999).

– *Labeling of T30S with cDNA*: The modified and the non-modified oligonucleotides were phosphorylated at the 5' end using $^{32}$P-P-ATP that allows following their binding to the T30S. This was checked by sucrose gradient centrifugation. The amount of bound oligomers was calculated from the amount of radioactivity that migrated together with the T30S peak on the gradient (Auerbach *et al.*, 1999).

– *Labeling of the oligomers with 3Cys*-TAMM: In order to avoid inter-molecular crosslinking, three of the four mercury atoms in the TAMM molecule were blocked before labeling the oligomers by incubating the TAMM with a three fold excess of $^{35}$S-cysteine. The use of $^{35}$S-cysteine as blocking reagent also allows monitoring the binding of the TAMM modified oligomers to the T30S subunits. The modified oligonucleotides were phosphorylated using T4 polynucleotide kinase prior to the labeling with TAMM (Auerbach *et al.*, 1999).

The position of the TIR and the TAMM compounds were determined as described in Weinstein *et al.* (1999).

**Acknowledgments** – Thanks are given to M. Wilchek for indispensable advice, to M. Safro for active participation in phasing, to W. Jahn, W. Preetz and M. Pope for their generous gifts of heavy atom compounds, to W. Traub for fruitful discussions, and to C. Radzwill, H. Burmeister, R. Albrecht, C. Glotz, J. Müssig, C. Paulke, M. Laschever, S. Meier, Y. Halfon and K. Knaack, for their excellent contributions in the different stages of these studies. Data were collected at the EMBL (BW7) and MPG beam lines at DESY (BW6); F1/CHESS, Cornell University (F1); ID2 and ID13 at ESRF, Grenoble (France) and ID19/APS at Argonne National Lab. (ID19). Support was provided by the Max-Planck Society (Germany), the US National Institute of Health (NIH GM 34360), the German Ministry for Science and Technology (BMBF 05-641EA) and the Kimmelman Center for Macromolecular Assembly at the Weizmann Institute (Rehovot, Israel). AY holds the Martin S. Kimmel Professorial Chair.

## REFERENCES

Alexander, R.W., Muralikrishna, P. and Cooperman, B.S., Ribosomal components neighboring the conserved 518-533 loop of 16S rRNA in 30S subunits. *Biochemistry* 1994, **33**: 12109-12118.

Auerbach, T., Pioletti, T., Avila, H., Anagnostopoulos, K., Weinstein S., Franceschi, F. and Yonath, A., Genetic and biochemical manipulation of the small ribosomal subunit from *T. thermophilus* HB8. *Biomol. Struct. Dyn.* 1999, **17**: 617-628.

Basavappa, R. and Sigler, P.B., The 3-dimensional structure of yeast initiator tRNA: functional implication in initiator/elongator discrimination. *EMBO J.* 1991, **10**: 3105-3110

Bashan, A., Pioletti, M., Bartels, H., Janell, D., Schluenzen, F., Gluehmann, M., Levin, I., Harms, J., Hansen, H.A.S., Tocilj, A., Auerbach, T., Avila, H., Anagnostopoulos, K., Simitsopoulou, M., Peretz, M., Bennett, W.S., Agmon, I., Kessler, M., Weinstein, S., Franceschi, F. and Yonath, A., The identification of selected ribosomal components in crystallographic maps of prokaryotic ribosomal subunits at medium resolution. *ASM Publ.* 1999, in press.

Bentley, G.A., Boulot, G., Riottot, M.M. and Poljak, R.J., Three-dimensional structure of an idiotype anti-idiotype

complex. *Nature* 1990, **348**: 254-257.

Berglund, H., Rak, A., Serganov, A., Garber, M. and Härd, T., Solution structure of the ribosomal RNA binding protein S15 from *Thermus thermophilus*. *Nat. struct. Biol.* 1997, **4**: 20-23.

Berkovitch-Yellin, Z., Bennett, W.S. and Yonath, A., Aspects in structural studies on ribosomes. *CRC Rev Biochem. mol. Biol.* 1992, **27**: 403-444.

Brimacombe, R., The structure of ribosomal RNA; a three-dimensional jigsaw puzzle. *Eur. J. Biochem.* 1995, **230**: 365-383.

Camp, D. and Hill, W.E., Probing *E. coli* 16S ribosomal-RNA with DNA oligomers to determine functional and structural characteristics of the highly conserved G(530) loop. *FASEB J.* 1987, **46**: 2221, abstract.

Capel, M.S., Kjeldgaard, M., Engelman, D.M. and Moore, P.B., Positions of S2, S13, S16, S17, S19 and S21 in the 30S ribosomal subunit of *E. coli*. *J. mol. Biol.* 1988, **200**: 65-87.

Clemons, W.M., Davies, C., White, S. and Ramakrishnan, V., Conformational variability of the N-terminal helix in the structure of ribosomal protein S15. *Structure* 1998, **6**: 429-438.

Cusack, S., Protein nucleic-acid complexes. *Curr. Opin. struct. Biol.* 1999, **9**: 66-73.

Davies, C., Ramakrishnan, V. and White, S.W., Structural evidence for specific S8-RNA and S8-protein interactions within the 30S ribosomal subunit: Ribosomal protein S8 from *Bacillus stearothermophilus* at 1.9 Å resolution. *Structure* 1996, **4**: 1093-1104.

Deisenhofer, J., Epp, O., Miki, K., Huber, R. and Michel, H., X-ray structure analysis of a membrane protein complex. Electron density map at 3 Å resolution and a model of the chromophors of the photosynthetic reaction center from rhodopseudomonos viridis. *J. mol. Biol.* 1984, **180**: 385-398.

Draper, D.E. and Reynoldo, L.P., RNA binding strategies of ribosomal proteins. *Nucl. Acid. Res.* 1999, **27**: 381-388.

Frank, J., Zhu, J., Penczek, P., Li, Y., Srivastava, S., Verschoor, A., Radermacher, M., Grassucci, R., Lata, A.R. and Agrawal, R.K., A model of protein synthesis based on cryo electron microscopy of the *E. coli* ribosome. *Nature* 1995, **376**: 441-444.

Gabashvili, I.S., Agrawal, R.K., Grassucci, R. and Frank, J., Structure and structural variations of the *E. coli* 30S ribosomal subunit as revealed by three-dimensional cryo-electron microscopy. *J. mol. Biol.* 1999, **286**: 1285-1291.

Gelasco, A. and Lippard, S.J., NMR solution structure of a DNA dodecamer duplex containing a cis-diamineplatinum(II) D(GPG) itrasrand cross-ling, the major adduct of the anticancer drug cis-platin. *Biochemistry* 1998, **37**: 9230-9239.

Golden, B.L., Hoffman, D.W., Ramakrishnan, V. and White, S.W., Ribosomal protein S17: characterization of the three-dimensional structure by H and N NMR. *Biochemistry* 1993, **32**: 12812-12820.

Harms, J., Tocilj, A., Levin, I., Agmon, I., Kölln, I., Stark, H., van Heel, M., Cuff, M., Schlünzen, F., Bashan, A., Franceschi, F. and Yonath, A., Elucidating the medium resolution structure of ribosomal particles: an interplay between electron-cryo-microscopy and X-ray crystallography. *Structure* 1999, **7**: 931-941.

Held, W.A., Ballou, B., Mizushima, S. and Nomura, M., Assembly mapping of 30S ribosomal proteins from *E. coli*. *Nature* 1974, **266**: 1214-1218.

Hosaka, H., Nakagawa, A., Tanaka, I., Harada, N., Sano, K., Kimura, M., Yao, M. and Wakatsuki, S., Ribosomal protein S7: a new RNA binding. *Structure* 1997, **5**: 1199-1208.

Jahn, W., Synthesis of water soluble tetrairidium cluster for specific labelling of proteins. *Z. Naturforsch.* 1989, **44b**: 79-82.

Krumbholz, S., Schlünzen, F., Harms, J., Bartels, H., Kölln, I., Knaack, K., Bennett, W.S., Bhanumoorthy, P., Hansen, H.A.S., Volkmann, N., Bashan, A., Levin, I., Tocilj, A. and Yonath, A., Ribosomal crystallography: cryo protectants and cooling agents. *Periodicum Biologorum* 1998, **100**: 119-125.

Lata, A.R, Agrawal, R.K., Penczek, P., Grassucci, R., Zhu, J. and Frank, J., Three-dimensional reconstruction of the *E. coli* 30S ribosomal in ice. *J. mol. Biol.* 1996, **262**: 43-52.

Liljas, A. and Al-Karadaghi, S., Structural aspects of protein synthesis. *Nat. struct. Biol.* 1997, **4**: 767-771.

Lindhal, M., Svensson, L.A., Liljas, A., Sedelnikova, S.E., Eliseukina, I., Fomenkova, N., Nevskaya, N., Nikonov, S., Garber, N. and Muranova, T.A., Crystal structure of the ribosomal protein S6 from *Thermus thermophilus*. *EMBO J.* 1994, **13**: 1249-1254.

Luger, K., Maeder, A.W., Richmond, R.K., Segent, D.F. and Richmond, T.J., Crystal structure of the nucleosome core particle at 2.8 Å resolution. *Nature* 1997, **389**: 251-260.

Merryman, C., Moazed, D., McWhirter, J. and Noller, H.F., Nucleotides in 16S rRNA protected by the association of 30S and 50S ribosomal subunits. *J. mol. Biol.* 1999, **285**: 97-105.

Moazed, D. and Noller, H.F., Interaction of antibiotics with functional sites in 16S ribosomal RNA. *Nature* 1987, **327**: 389-394.

Mueller, F. and Brimacombe, R., A new model of the three-dimensional folding of *E. coli* 16S ribosomal RNA. II. RNA-protein interaction data. *J. mol. Biol.* 1997, **271**: 524-544.

Nevskaya, N., Tishchenko, S., Nikulin, A., Al-Karadaghi, S., Liljas, A., Ehresmann, B., Ehresmann, C., Garber, M. and Nikonov, S., Crystal structure of ribosomal protein S8 from *Thermus thermophilus* reveals a high degree of structural conservation of a specific RNA binding site. *J. mol. Biol.* 1998, **279**: 233-244.

Oakes, M.I., Clark, M.W., Henderson, E. and Lake, J.A., DNA hybridization electron microscopy: ribosomal RNA nucleotides 1392-1407 are exposed in the cleft of the small subunit. *Proc. natn. Acad. Sci.* USA 1986, **83**(2): 275-279.

Ramakrishnan, V. and White, S.W., The structure of ribosomal protein S5 reveals sites of interaction with 16S RNA. *Nature* 1992, **358**: 768-771.

Ramakrishnan, V. and White, S.W., Ribosomal protein structures: insights into the architecture, machinery and evolution of the ribosome. *TIBS* 1998, **3**: 208-212.

Reeder, F., Guo, Z.J., Murdoch, P.D., Corazza, A., Hambley, T.W., Bernersprice, S.J., Chottard, J.C. and Sadler, P.J.,

Platination of a GG site on single-stranded and double-stranded forms of a 14-basy oligonucleotide with diaqua cisplatin followed by NMR and HPLC - influence of the Pt ligand and base sequence on 5'-G versus 3'-G platination selectivity. *Eur. J. Biochem.* 1997, **249**: 370-382.

Reinemer, P., Dirr, H.W., Ladenstein, R., Schaeffer, J., Gallay, O. and Huber, R., The three dimensional structure of class II glutathione S-transferase in complex with glutathione sulfonate at 2.3 Å resolution. *EMBO J.* 1991, **10**: 1997-2005.

Richmond, T.J., Finch, J.T., Rushton, B., Rhodes, D. and Klug, A., Structure of the nucleosome core particle at 7 Å resolution. *Nature* 1984, **311**: 532-537.

Ricker, R.D. and Kaji, A., Use of single strand DNA oligonucleotide in programming ribosomes for translation. *Nucl. Acid Res.* 1991, **19**: 6573-6578.

Sagi, I., Weinrich, V., Levin, I., Glotz, C., Laschever, M., Melamud, M., Franceschi, F., Weinstein, S. and Yonath, A., Crystallography of ribosomes: Attempts at decorating the ribosomal surface. *Biophys. J.* 1995, **55**: 31-41.

Schluenzen, F., Gluehmann, M., Janell, D., Levin, I., Bashan, A., Harms, J., Bartels, H., Auerbach, T., Pioletti, T., Avila, H., Anagnostopoulos, K., Hansen, H.A.S., Bennett, W.S., Agmon, I., Kessler, M., Tocilj, A., Peretz, M., Weinstein, S., Franceschi, F. and Yonath, A., The identification of selected components in electron density maps of prokaryotic ribosomes at 7 Å resolution. *J. Synchrotron Rad.* 1999, **6**: 928-941.

Schluenzen, F., Hansen, H.A.S., Thygesen, J., Bennett, W.S., Volkmann, N., Levin, I., Harms, J., Bartels, H., Bashan, A., Berkovitch-Yellin, Z., Sagi, I., Franceschi, F., Krumbholz, S., Geva, M., Weinstein, S., Agmon, I., Boeddeker, N., Morlang, S., Sharon, R., Dribin, A., Peretz, M., Weinrich, V. and Yonath, A., A milestone in ribosomal crystallography: the construction of preliminary electron density maps at intermediate resolution. *J. Biochem. Cell Biol.* 1995, **73**: 739-749.

Simitsopoulou, M., Avila, H. and Franceschi, F., Ribosomal Gene disruption in the extreme thermophilic *Thermus thermophilus*: generation of a mutant lacking ribosomal protein S17. *Eur. J. Biochem.* 1999, **266**: 524-532.

Stark, H., Mueller, F., Orlova, E.V., Schatz, M., Dube, P., Erdemir, T., Zemlin, F., Brimacombe, R., and van Heel, M., The 70S *E. coli* ribosome at 23 Å resolution: fitting the ribosomal RNA. *Structure* 1995, **3**: 815-821.

Stöffler, G. and Stöffler-Meilicke, M., Immuno electron microscopy on *E. coli* ribosomes. In: *Structure, Function and Genetics of Ribosomes*, Hardesty, B. and Kramer, G. (eds.), Springer Verlag, Heidelberg, 1986, pp. 28-46.

Szer, W. and Kurylo-Borowska, Z., Interactions of edeine with bacterial ribosomal subunits. Selective inhibition of aminoacyl-tRNA binding sites. *Biochem. biophys. Acta* 1972, **259**: 357-368.

Tanaka, I., Nakagawa, A., Hosaka, H., Wakatsuki, S., Mueller, F. and Brimacombe, R., Matching the crystallographic structure of ribosomal protein S7 to the 3D model of 16S RNA. *RNA* 1998, **4**: 542-550.

Tapprich, W.E. and Hill, W.E., Involvement of bases 787-795 of *E. coli* 16S RNA in ribosomal subunit association. *Proc. natn. Acad. Sci.* USA 1988, **83**: 556-560.

Tocilj, A., Schlünzen, F., Janell, D., Glühmann, M., Hansen, H.R.S., Harms, J., Bashan, A., Bartels, H., Agmon, I., Franceschi, F. and Yonath, A., The small ribosomal subunit from *Thermus thermophilus* at 4.5 Å resolution: patteen fitting and the identification of functional sites. *PNAS* 1999, **96**: 14252-14257.

Trakhanov, S.D., Yusupove, M.M., Shirokov, V.A., Garber, M.B., Mitscher, A., Ruff, M., Tierry, J.-C. and Moras, D., Preliminary X-ray investigation on 70S ribosome crystals. *J. mol. Biol.* 1989, **209**: 327-334.

Wada, T., Yamazaki, T., Kuramitsu, S. and Kyogoku, Y., Cloning of the RNA polymerase alfa subunit gene from *Thermus thermophilus* HB8 and characterization of the protein. *J. Biochem.* 1999, **125**: 143-150.

Wang, R., Alexander, R.W., VanLoock, M., Vladimirov, S., Bukhtiyarov, Y., Harvey, S.C. and Cooperman, B.S., Three-dimensional placement of the conserved 530 loop of 16 S rRNA and of its neighboring components in the 30 subunit, *J. mol. Biol.* 1999, **286**: 521-540.

Weinstein, S., Jahn, W., Glotz, C., Schlünzen, F., Levin, I, Janell, D., Harms, J., Kölln, I., Hansen, H.A.S., Glühmann, M., Bennett, W.S., Bartels, H., Bashan, A., Agmon, I., Kessler, M., Pioletti, M., Avila, H., Anagnostopoulos, K., Peretz, M., Auerbach, T., Franceschi, F. and Yonath, A., Metal compounds as tools for the construction and the interpretation of medium resolution maps of ribosomal particles. *J. Struct. Biol.* 1999, **127**: 141-151.

Weller, J.W. and Hill, W.E., Probing dynamic changes in rRNA conformation in the 30S subunit of the *E. coli* ribosome. *Biochemistry* 1992, **31**: 2748-2757.

Wimberly, B.T., White, S.W. and Ramakrishnan, V., The structure of ribosomal protein S7 as 1.9 Å resolution reveals a b-hairpin motif double stranded nucleic acids. *Structure* 1997, **5**: 1187-1198.

Yonath, A., Glotz, C., Gewitz, H.S., Bartels, K., von Boehlen, K., Makowski, I. and Wittmann, H.G., Characterization of crystals of small ribosomal subunits. *J. mol. Biol.* 1988, **203**: 831-833.

Yonath, A., Harms, J., Hansen, H.A.S., Bashan, A., Peretz, M., Bartels, H., Schluenzen, F., Koelln, I., Bennett, W.S., Levin, I., Krumbholz, S., Tocilj, A., Weinstein, S., Agmon, I., Piolleti, M., Auerbach, T. and Franceschi, F., The quest for the molecular structure of a large macromolecular assembly exhibiting severe non-isomorphism, extreme beam sensitivity and no internal symmetry. *Acta Crystal.* 1998, **54A**: 945-955.